VERSITA

OPTO-ELECTRONICS REVIEW **14**(3), 205–211

DOI: 10.2478/s11772-006-0027-8

$Tb_3Sc_2Al_3O_{12}$-$TbScO_3$ eutectic self-organized microstructure for metamaterials and photonic crystals application

K. KOŁODZIEJAK[1], S. TURCZYŃSKI[1,2], R. DIDUSZKO[1], L. KLIMEK[2], and D.A. PAWLAK*[1]

[1]Institute of Electronic Materials Technology, 133 Wólczyńska Str., 01-919 Warsaw, Poland
[2]Institute of Materials Science and Engineering, Technical University of Łódź, 1/15 Stefanowskiego Str., 90-924 Łódź, Poland

Eutectics are the materials with foreseen application in the field of photonic crystals and metamaterials. In this paper, the dependence on chemical composition of the microstructures of terbium-scandium-aluminium garnet and terbium-scandium perovskite ($Tb_3Sc_2Al_3O_{12}$-$TbScO_3$) eutectics has been studied. The growth of the eutectic rods by the micro-pulling down method is presented, using compositions with several different volume fractions of the garnet and the perovskite phases, V_{TSAG}:V_{TSP} = 4, 3, 2, 1, 1/2. The phases have been characterized by powder X-ray diffraction and energy dispersive spectrometry. The relationship between the lattice constant of individual phases and the chemical composition is presented. The unidirectional growth of microrods has been also investigated by electron backscattering diffraction.

Keywords: eutectic, micro-pulling down method, oxide, $TbScO_3$, $Tb_3Sc_2Al_3O_{12}$, microstructure.

1. Introduction

The self-organized micro- and nanostructured eutectic materials obtained by the directional solidification could be used for various types of light manipulation. Until recently, eutectics were mainly studied as structural materials because of their excellent mechanical properties. Mostly metal-metal eutectics were studied for this reason, but more recently, various studies of oxide-oxide eutectics [1–5] have begun to appear in the literature. Oxide-oxide eutectics have also been a recent focus of research into optical materials [6,7] and have been identified as materials which may act as photonic crystals [8,9]. The next foreseen [10] potential application is in the field of metamaterials. Photonic crystals [11–14] and metamaterials [15–19] are widely being seen as exciting growth areas in photonics research.

Depending on different factors, such as the entropy of melting of both phases, eutectics can form micro- and nanostructures with diverse geometries. They can have regular-lammelar, regular-rod-like, irregular, complex regular, quasi-regular, broken-lamellar, spiral, and globular geometry. The regular shape seems to be well-suited for the photonic crystal application. The lammelar shape would be more appropriate for one-dimensional crystals, and the rod-like shape for two-dimensional crystals. The irregular or complex-regular shape as kind of percolated structures may have potential in the field of metamaterials, for example, in creating materials with giant dielectric constant [20]. The rare spiral geometry might be utilized in chiral metamaterials which could show negative refraction [18]. Finally, the rare globular-shaped eutectics, when grown as metalo-dielectric materials, may become invisible materials [21] or find application as plasmon-tunable materials [22].

Experimental data for oxide-oxide eutectics or hybrid eutectics as metal-oxide or semiconductor-oxide is still very limited. The oxide-oxide eutectics have properties that normally can make them well-suited as optical materials. This is because the individual phases of the eutectic are usually transparent over a wide range of wavelengths, and can also impart other useful properties to the eutectics. In the bunch of microfibers/microrods, formed in the fibrous/rodlike eutectic, light may propagate in a controlled way. For example, if the microrods were made of a material showing the Faraday effect, the light in the microrods would not only propagate but also the plane of linearly polarized light would be rotated in the presence of a magnetic field. If the materials, from which the microrods are made, were doped with active element, amplification of light may be possible. For non-linear materials, non-linear optical effects would be expected.

It was recently shown that the $Tb_3Sc_2Al_3O_{12}$-$TbScO_3$ eutectic tends to grow with a rodlike microstructure at the edge of the $Tb_3Sc_2Al_3O_{12}$ fibres grown by the micro-pulling down method [8]. In this paper, the growth of the $Tb_3Sc_2Al_3O_{12}$-$TbScO_3$ eutectic is explored with different volume ratios of the phases, in an attempt to generate rodlike microstructure in the whole of the grown eutectic bi-crystal.

*e-mail: Dorota.Pawlak@itme.edu.pl

2. Experimental procedure

2.1. Crystal growth

The eutectic bi-crystals were grown using a micro-pulling down method (m-PD). The m-PD method was invented in Japan, originally for growth of single crystal fibres [23–26]. The growth of oxide-oxide eutectics for high strength materials has been already reported by this method [2,3,27]. The m-PD method utilises a crucible with a die at the bottom in which there is a centrally-placed nozzle. The raw materials are melted in the crucible, the melt passes through the nozzle, is touched with the seed crystal, and the crystal is then pulled down. Figure 1 shows the scheme of the thermal system used in all the experiments reported here. High purity oxide powders (99.995%), Tb_4O_7, Sc_2O_3, Al_2O_3, and Pr_6O_{11} were used as starting materials. The oxides were mixed with ethanol in alumina mortar and then dried. The crystals were grown with 0.15 mm/min pulling rate under a nitrogen atmosphere. The crystals grown were seeded with a <111> $Y_3Al_5O_{12}$ single crystal. The individual phases have been identified using powder X-ray diffraction and energy dispersive spectroscopy. A fully-aligned eutectic structure can be obtained only when the crystal/melt interface is flat. The other necessary conditions are, a steep temperature gradient, slow growth rate, and absence of convection [28,29]. All these conditions can probably be fulfilled by the m-PD method.

2.2. X-ray diffraction

X-ray powder diffraction measurements were performed on the as-grown samples using a Siemens D500 diffractometer equipped with semiconductor Si: Li detector, cooled with liquid nitrogen, and K_αCu radiation (λ = 1.5418 Å). The powder diffraction pattern was measured in $\theta/2\theta$ scanning mode with a step of 0.02° and an integration time of 10 sec/step. The experimental data were analyzed by Young DBWS-9807 program package [30].

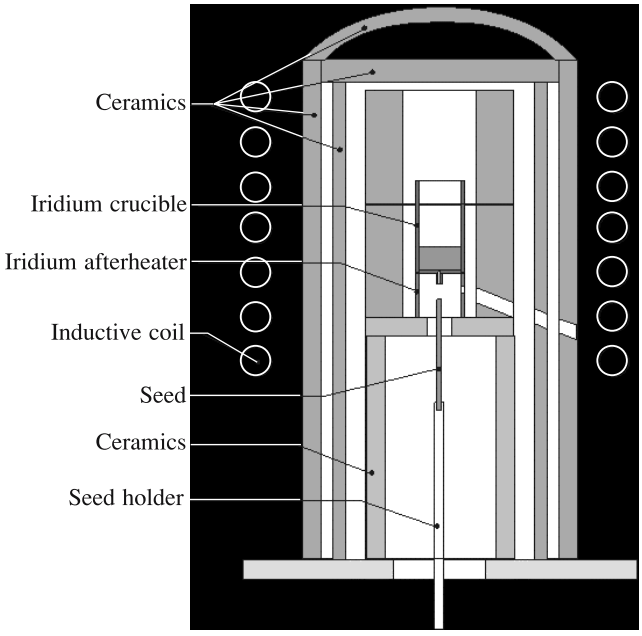

Fig. 1. Scheme of the thermal system used for all the experiments by the micro-pulling down method described in the paper.

2.3. Scanning electron microscopy measurements

The chemical composition of particular phases of obtained eutectic bi-crystals has been examined by a thermo NORAN scanning electron microscopy (SEM) equipped with energy dispersive spectrometer (EDS). The *e* orientation of the adjacent microrods has been investigated by the electron back-scattering diffraction (EBSD). The measurements were performed on HITACHI S3000N scanning electron microscopy. For the SEM, EDS, and EBSD measurements the (non-conductive) samples have been covered with thin layer of carbon, using BAL-TEC SCD 005 equipment at 10^{-2} mmBar of argon.

3. Results and discussion

In this work, the eutectic crystals of terbium-scandium-aluminium garnet – terbium-scandium perovskite, $Tb_3Sc_2Al_3O_{12}$ (TSAG)-$TbScO_3$ (TSP), were grown by the micro-pulling down method. They were grown in the form of crystal rods of 3 mm in the diameter and they were usually longer than 10 cm. The eutectic rods were grown with the following ratios of the two phases, V_{TSAG}:V_{TSP} = 4, 3, 2, 1, 1/2. The applied pulling rate was 0.15 mm/min in all cases.

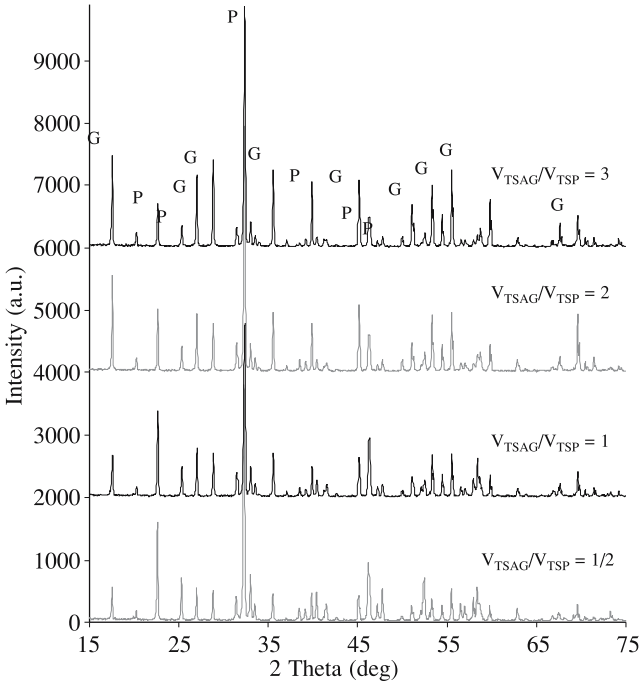

Fig. 2. Powder X-ray diffraction pattern for the $Tb_3Sc_2Al_3O_{12}$-$TbScO_3$ eutectic grown with different volume fractions of their phases, V_{TSAG}:V_{TSP} = 3, 2, 1, 1/2.

The presence of different phases has been checked by powder X-ray diffraction measurements. Figure 2 shows the diffractograms for the samples grown from compositions with different volume ratios of both phases, V_{TSAG}:V_{TSP} = 3, 2, 1, 1/2. Only these two phases were found: terbium-scandium-aluminium garnet and terbium-scandium perovskite. When the volume fraction of the garnet (TSAG) phase increases and the volume fraction of perovskite phase decreases, the intensity of the garnet phase peaks increases and the intensity of the perovskite peaks decreases, Fig. 2.

The lattice parameters were calculated using Rietveld analysis and they are given in Table 1. With the increase in concentration of the perovskite phase in the grown rods, and a concomitant increase in the amount of perovskite dendrites, the lattice constants of the perovskite increase slightly. The lattice constant of the garnet phase, on the other hand, seems to behave in an irregular manner.

Table 1. Lattice parameters of the $Tb_3Sc_2Al_3O_{12}$ (TSAG) and $TbScO_3$ (TSP) phases in the grown eutectic rods.

$Tb_3Sc_2Al_3O_{12}$-$TbScO_3$ eutectic crystals	Lattice parameter (Å)			
	Perovskite phase			Garnet phase
	a	b	c	a
V_{TSAG}:V_{TSP} = 3	5.4312	5.6861	7.8533	12.3866
V_{TSAG}:V_{TSP} = 2	5.4313	5.6877	7.8492	12.3858
V_{TSAG}:V_{TSP} = 1	5.4314	5.6901	7.8543	12.3863
V_{TSAG}:V_{TSP} = 1/2	5.4320	5.6912	7.8540	12.3876

The diffraction data were also used to calculate the mass fraction of the individual phases. In Table 2, the calculated data is compared with the expected mass fractions – based on the weighed materials during the preparation step. The X-ray calculated and expected mass fractions are generally very similar.

Energy dispersive spectrometry (EDS) has been used to identify the particular phases on the SEM images with the garnet or perovskite phase. The dark phase has been identified as the garnet phase and the light grey phase has been identified as the perovskite phase. In Table 3, the quantities of each element are shown for a sample additionally doped with praseodymium. Carbon comes from the carbon layer with which the samples were covered in order to take away the charge from the isolating samples during the measurements.

Table 3. Atomic percentage of elements in $Tb_3Sc_2Al_3O_{12}$-$TbScO_3$ grown from composition V_{TSAG}:V_{TSP} = 2 doped with 5 at. % Pr ions.

Elements	% of the element in dark grey phase – garnet phase	% of the element in light grey phase – perovskite phase
Carbon	30.10	34.51
Oxygen	40.67	36.38
Aluminium	10.26	2.04
Scandium	7.38	12.69
Praseodymium	0.20	0.56
Terbium	11.39	13.81

Figure 3 depicts the results of a linear analysis of chemical composition using EDS. The arrow on the right-hand picture indicates the part of the sample where the analysis was carried out. It can be seen that in the light-coloured phase, the scandium has much higher concentration and that the concentration of aluminium is much smaller. This clearly shows that the grey phase is $TbScO_3$. In the case of the dark phase, the concentration of scandium is decreased and the concentration of aluminium is increased, which proves that this is a $Tb_3Sc_2Al_3O_{12}$ phase.

Figure 4 show the general (small magnification) SEM images of the cross-section and longitudinal section of grown eutectic rods.

In the case when there is a relatively small fraction of $TbScO_3$ phase (V_{TSAG}:V_{TSP} = 4) there is not enough of this phase in the rod, and the eutectic grows beyond the rod perimeter; inside there is a single crystal of the $Tb_3Sc_2Al_3O_{12}$ phase. When the fraction of $TbScO_3$ phase is slightly increased (V_{TSAG}:V_{TSP} = 3) the eutectic exists in all of the as-grown rod, but the microstructure is not consistently the rodlike one, Fig 4(a). When the volume fraction of $TbScO_3$ phase increases still further (V_{TSAG}:V_{TSP} = 2) there seems to be already too much of the perovskite phase, since in the centre of the eutectic rod dendrites of this phase start to ap-

Table 2. Comparison of $Tb_3Sc_2Al_3O_{12}$ and $TbScO_3$ mass fractions.

$Tb_3Sc_2Al_3O_{12}$-$TbScO_3$ eutectic crystals	$Tb_3Sc_2Al_3O_{12}$-$TbScO_3$ mass fractions (calculated, based on the X-ray diffraction)	$Tb_3Sc_2Al_3O_{12}$-$TbScO_3$ mass fractions (assumed data, based on the weighed raw materials)
V_{TSAG}:V_{TSP} = 3	69.5–30.5%	72.8–27.2%
V_{TSAG}:V_{TSP} = 2	59.2–40.8%	64.0–36.0%
V_{TSAG}:V_{TSP} = 1	49.7–50.3%	47.1–52.9%
V_{TSAG}:V_{TSP} = 1/2	36.5–63.5%	30.8–69.2%

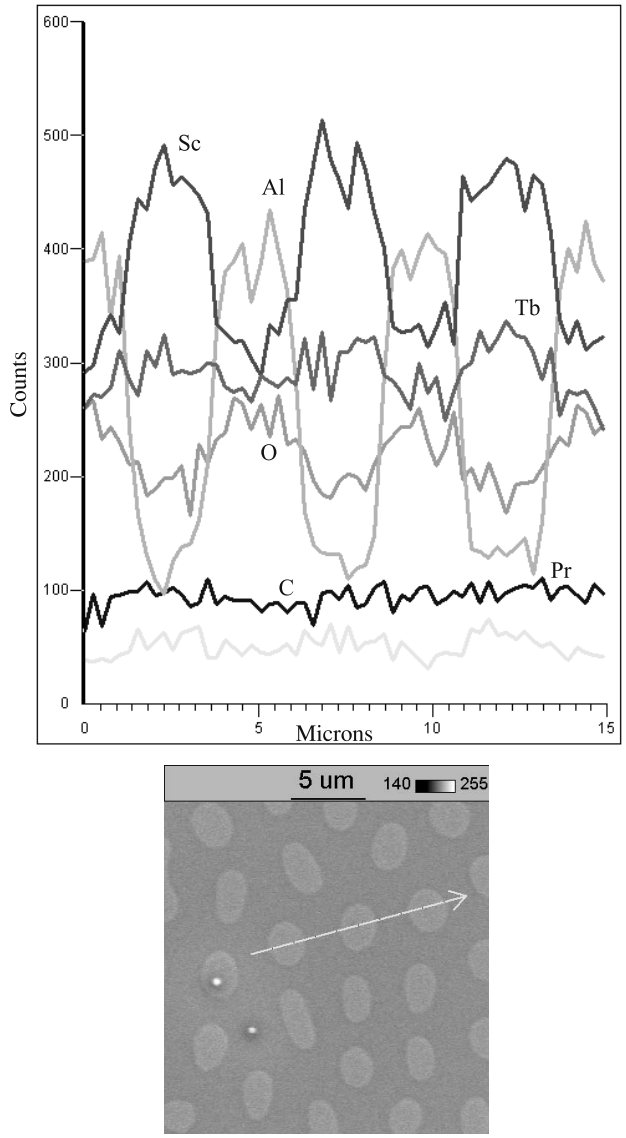

Fig. 3. Linear EDS analysis of chemical composition of $Tb_3Sc_2Al_3O_{12}$-$TbScO_3$:Pr (5 at. %) eutectic (V_{TSAG}:V_{TSP} = 2).

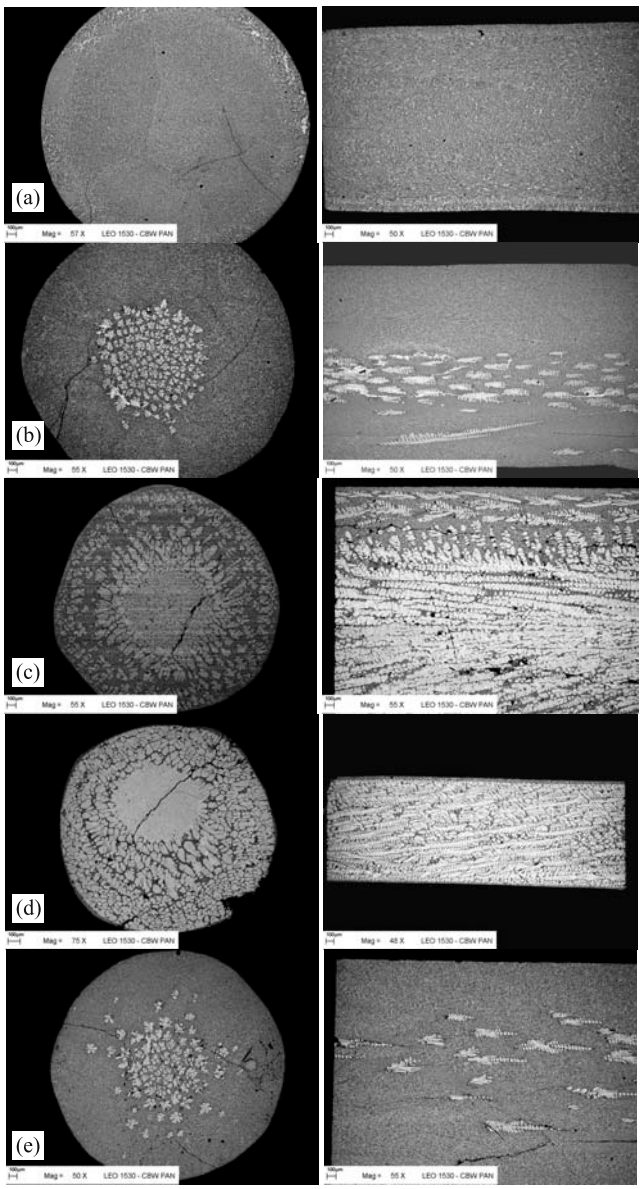

Fig. 4. SEM images of the cross-section (left) and longitudinal section (right) of $Tb_3Sc_2Al_3O_{12}$-$TbScO_3$ eutectic obtained with 15 mm/min pulling rate and grown from compositions of different volume ratios of its phases, (a) $V_{TSAG}/V_{TSP} = 3$, (b) $V_{TSAG}/V_{TSP} = 2$, (c), (d) $V_{TSAG}/V_{TSP} = 1/2$, and (e) $V_{TSAG}/V_{TSP} = 2 + 5$ at. % Pr (the perovskite phase is grey, the garnet phase is black). The contrast is generated by different phases relative to their average atomic number.

pear, Fig 4(b). In Fig. 5, these dendrites are shown with higher magnification. They are surrounded by the rodlike eutectic microstructure, which also appears in most of the rest of the eutectic rod. In Fig. 6, the rodlike microstructure in the eutectic grown from a composition V_{TSAG}:V_{TSP} = 2 is shown in the cross-section and longitudinal section.

In the rods grown with even higher fraction of the perovskite phase, e.g., V_{TSAG}:V_{TSP} = 1, many more dendrites of the perovskite phase are formed, Fig. 4(c). In the case of the composition V_{TSAG}:V_{TSP} = 1/2, the perovskite dendrites overgrown the whole rod, Fig. 4(d). From the grown compositions we identify the $Tb_3Sc_2Al_3O_{12}$-$TbScO_3$ eutectic with the volume ratio of V_{TSAG}:V_{TSP} = 2 as the best composition for obtaining the rodlike microstructure, with only small fraction of $TbScO_3$ dendrites.

In all eutectics, which we investigate until now, there was always a matrix, in which the whole rod grew in one well-defined crystallographic direction. In these materials, it appears that some disturbances in the growth prevent the formation of a homogenous microstructure, and consequently the phase forming the micro-pattern does not show one distinguished direction in the whole eutectic rod. It has been shown for $Tb_3Sc_2Al_3O_{12}$-$TbScO_3$ eutectics, using single crystal X-ray diffraction from a crystal plane perpendicular to the growth direction, that the matrix phase, i.e., the garnet phase – grows in <111> direction while the perovskite phase does not seem to show a distinguished direction of growth [10]. In order to see if this might be a result of the inhomogeneity, homogeneity of the obtained eu-

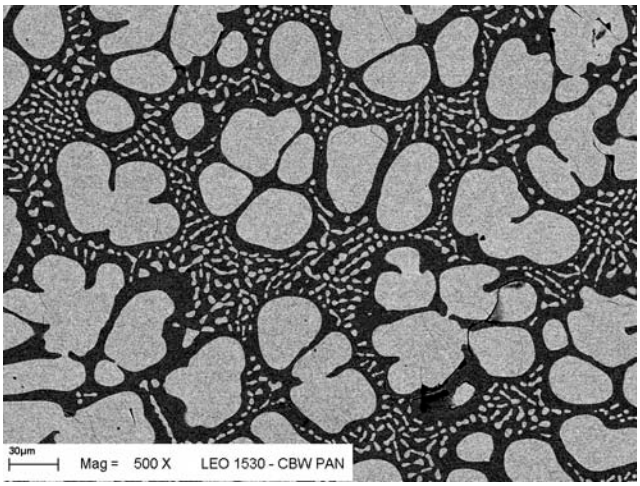

Fig. 5. SEM images of dendrites of the $TbScO_3$ phase which appear in the $Tb_3Sc_2Al_3O_{12}$-$TbScO_3$ eutectic with the volume ratio $V_{TSAG}/V_{TSP} = 2$.

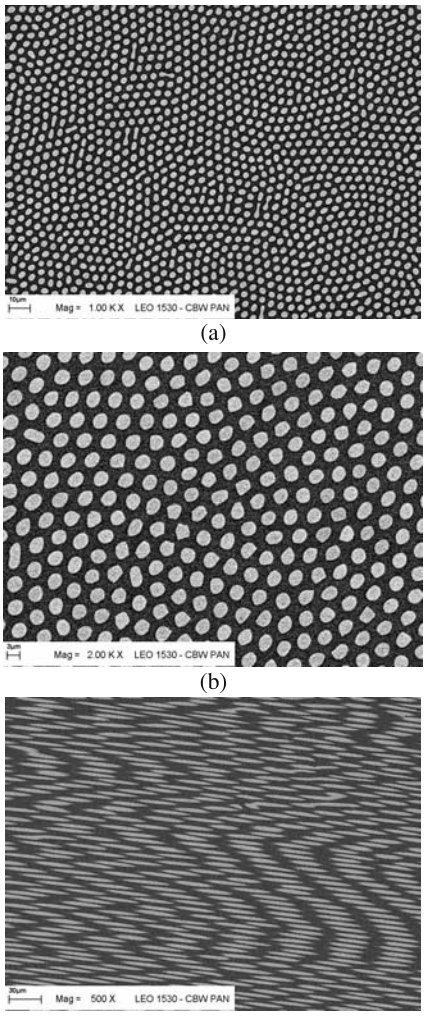

Fig. 6. Self-organized pseudo-hexagonally packed $Tb_3Sc_2Al_3O_{12}$-$TbScO_3$ ($V_{TSAG}/V_{TSP} = 2$) eutectic microstructure obtained with 15 mm/min pulling rate: (a), (b) cross-section, and (c) longitudinal section (the perovskite phase is grey, the garnet phase is black).

tectics, electron backscattering diffraction measurements have been preformed on two samples. In each sample, nine different adjacent perovskite microrods were selected for the measurements. In Fig. 7, the measurements for one of the samples are presented. Figure 7(a) shows the measurement area observed by SEM and Fig. 7(b) shows the electron backscattering diffraction from the perovskite microrods (light grey areas) indicated by numbers in Fig 7(a). In both cases, the diffraction pattern is identical for all nine of the investigated adjacent perovskite microrods. This proves that in some large areas where the fibres grow in a similar direction, the crystallographic orientation of the perovskite phase is also the same in these microrods.

4. Conclusions

The eutectic rods were grown by the micro-pulling down method from compositions with different volume fractions of the garnet : perovskite phases, V_{TSAG}:V_{TSP} = 4, 3, 2, 1, 1/2. The dependence of the microstructure of terbium-scandium-aluminium garnet and terbium-scandium perovskite eutectic on the chemical composition has elucidated. Upon increase in the fraction of the perovskite phase, $TbScO_3$ dendrites are formed, initially in the centre of the eutectic rod, and (with even higher perovskite concentration) then tending to occupy the whole rod. From the investigated compositions, the ratio V_{TSAG}:V_{TSP} = 2 leads to the fibrous eutectic structure and the smallest amount of perovskite dendrites in the centre. Arguably, there is scope for further investigations close to this composition, in order to find an "optimal" composition when the $TbScO_3$ dendrites are not formed at all. In the homogenous parts of the eutectic, adjacent microfibres grow in the same crystallographic orientation.

Acknowledgments

The authors thank the Ministry of Scientific Research and Information Technology of Poland for support of this work (grant No. 4 T11B 015 24). The authors would like to acknowledge the Network of Excellence, METAMORPHOSE (No. 500252) and Dr Siân Howard (University of South Australia) for a critical reading of the manuscript.

References

1. Y. Waku, N. Nakagawa, T. Wakamoto, H. Ohtsubo, K. Shimizu, and Y. Kohtoku, "A ductile ceramic eutectic composite with high strength at 1873 K", *Nature* **389**, 49–52 (1997).
2. J.H. Lee, A. Yoshikawa, S.D. Durbin, D.H. Yoon, T. Fukuda, and Y. Waku, "Microstructure of Al_2O_3/ZrO_2 eutectic fibers grown by the micro-pulling down method", *J. Cryst. Growth* **222**, 791–796 (2001).
3. J.H. Lee, A. Yoshikawa, H. Kaiden, K. Lebbou, T. Fukuda, D.H. Yoon, and Y. Waku, "Microstructure of Y_2O_3 doped Al_2O_3/ZrO_2 eutectic fibers grown by the micro-pulling-down method", *J. Cryst. Growth* **231**, 179–185 (2001).

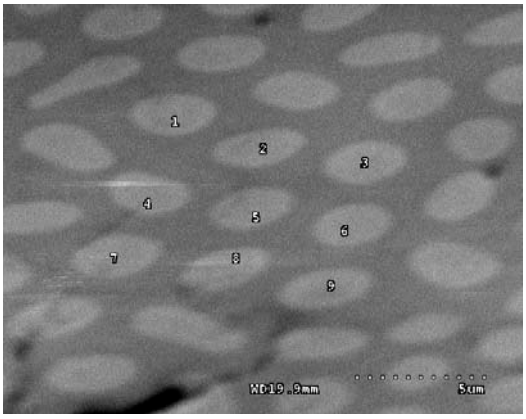

(a)

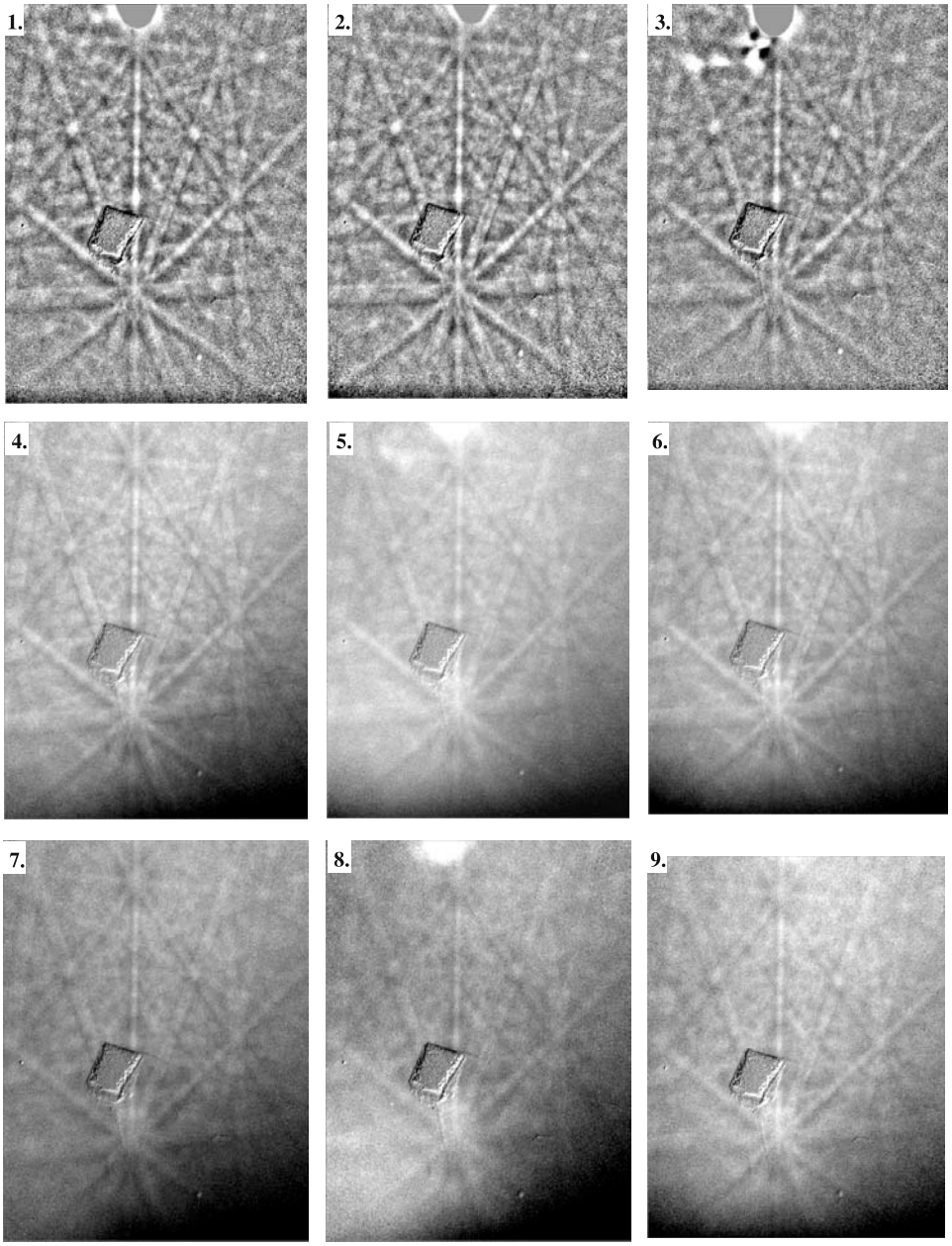

(b)

Fig. 7. The area of the $Tb_3Sc_2Al_3O_{12}$-$TbScO_3$:Pr (5 at.%) eutectic (V_{TSAG}:V_{TSP} = 2) where electron back-scattered diffraction measurement were made. The numbers label the particular perovskite microfibres from which the measurement has been taken (a). The electron back-scattered diffraction of perovskite microfibres from $Tb_3Sc_2Al_3O_{12}$-$TbScO_3$:Pr (5 at. %) eutectic (V_{TSAG}:V_{TSP} = 2) (b).

4. N. Nakagawa, H. Ohtsubo, A. Mitani, K. Shimizu, and Y. Waku, "High temperature strength and thermal stability for melt growth composite", *J. Eur. Ceramic Soc.* **25**, 1251–1257 (2005).
5. J. Llorca, and V.M. Orera, "Directionally solidified eutectic ceramic oxides", *Progress in Mat. Science* **51**, 711–809 (2006).
6. R.I. Merino, J.A. Pardo, J.I. Peña, G.F. de la Fuente, A. Larrea, and V.M. Orera, "Luminescence properties of ZrO_2-CaO eutectic crystals with ordered lamellar microstructure activated with Er^{3+} ions", *Phys. Rev.* **B56**, 10907–10915 (1997).
7. V.M. Orera, J.I. Peña, R.I. Merino, J.A. Lázaro, J.A. Vallés, and M.A. Rebolledo, "Prospects of new planar optical waveguides based on eutectic microcomposites of insulating crystals. The ZrO_2(c)-$CaZrO_3$ erbium doped system", *Appl. Phys. Lett.* **71**, 2746–2748 (1997).
8. D.A. Pawlak, G. Lerondel, I. Dmytruk, Y. Kagamitani, S. Durbin, and T. Fukuda, "Second order self-organized pattern of terbium-scandium-aluminum garnet and terbium-scandium perovskite eutectic", *J. Appl. Phys.* **91**, 9731–9736 (2002).
9. R.I. Merino, J.I. Pena, A. Larrea, G.F. de la Fuente, and V.M. Orera, "Melt grown composite ceramics obtained by directional solidification: structural and functional applications", *Recent Res. Devel. Mat. Sci.* **4**, 1–24 (2003).
10. D.A. Pawlak, K. Kołodziejak, S. Turczynski, J. Kisielewski, K. Rożniatowski, R. Diduszko, M. Kaczkan, and M. Malinowski, "Self-organized, rod-like, micron-scale microstructure of $Tb_3Sc_2Al_3O_{12}$-$TbScO_3$:Pr eutectic", *Chem. Mat.* **18**, 2450–2457 (2006).
11. S. John, "Strong localization of photons in certain disordered dielectric superlattices", *Phys. Rev. Lett.* **58**, 2486–2489 (1987).
12. E. Yablonowitch, "Inhibited spontaneous emission in solid-state physics and electronics", *Phys. Rev. Lett.* **58**, 2059–2062 (1987).
13. J.D. Joannopoulos, P.R. Villeneuve, and S. Fan, "Photonic crystals: putting a new twist on light", *Nature* **386**, 143–149 (1997).
14. A. von Blaaderen, "Opals in a new light", *Science* **282**, 887–888 (1998).
15. J.B. Pendry, "Negative refraction makes a perfect lens", *Phys. Rev. Lett.* **85**, 3966–3969 (2000).
16. R. Shelby, D.R. Smith, and S. Schultz, "Experimental verification of a negative index of refraction", *Science* **292**, 77–79 (2001).
17. S. Linden, C. Enkrich, M. Wegener, J. Zhou, T. Koschny, and C.M. Soukoulis, "Magnetic response of metamaterials at 100 terahertz", *Science* **306**, 1351–1353 (2004).
18. J.B. Pendry, "A chiral route to negative refraction", *Science* **306**, 1353–1355 (2004).
19. N. Fang, H. Lee, Ch. Sun, and X. Zhang, "Sub-diffraction-limited optical imaging with a silver superlens", *Science* **308**, 534–537 (2005).
20. C. Pecharroman, F. Esteban-Betegon, J.F. Bartolome, S. Lopez-Esteban, and J.S. Moya, "New percolative $BaTiO_3$-Ni composites with a high and frequency-independent dielectric constant (εr ≈80000)", *Adv. Mater.* **13**, 1541–1544 (2001).
21. F.J. Garcia de Abajo, G. Gomez-Santos, L.A. Blanco, A.G. Borisov, and S.V. Shabanov, "Tunneling mechanism of light transmission through metallic films", *Phys. Rev. Lett.* **95**, 067403-1-4 (2005).
22. S. Riikonen, I. Romero, and F.J. Garcia de Abajo, "Plasmon tunability in metallodielectric metamaterials", *Phys. Rev.* **B71**, 235104-1-6 (2005).
23. D.H. Yoon, I. Yonenaga, N. Ohnishi, and T. Fukuda, "Crystal growth of dislocation-free $LiNbO_3$ single crystals by micro pulling down method", *J. Cryst. Growth* **142**, 339–343 (1994).
24. Y.M. Yu, V.I. Chani, K. Shimamura, K. Inaba, and T. Fukuda, "Growth of vanadium garnet fiber crystals and variations of lattice parameter", *J. Cryst. Growth* **177**, 74–78 (1997).
25. D.A. Pawlak, Y. Kagamitani, A. Yoshikawa, K. Wozniak, H. Sato, H. Machida, and T. Fukuda, "Growth of Tb-Sc-Al garnet single crystals by the micro-pulling down method", *J. Cryst. Growth* **226**, 341–347 (2001).
26. V.I. Chani, A. Yoshikawa, H. Machida, and T. Fukuda, "Melt growth of $(Tb,Lu)_3Al_5O_{12}$ mixed garnet fiber crystals", *J. Cryst. Growth* **212**, 469–475 (2000).
27. A. Yoshikawa, K. Hasegawa, J.H. Lee, S.D. Durbin, B.M. Epelbaum, D.H. Yoon, T. Fukuda, and Y. Waku, "Phase identification of Al_2O_3/$RE_3Al_5O_{12}$ and Al_2O_3/$REAlO_3$ (RE = Sm-Lu, Y) eutectics", *J. Cryst. Growth* **218**, 67–73 (2000).
28. R.L. Ashbrook, "Directionally solidified ceramic eutectics", *J. Am. Cer. Soc.* **60**, 428–435 (1977).
29. F.R. Mollard, and M.C. Flemings, "Growth of composites from the melt: II", *Trans AIME* **239**, 1534–1546 (1967).
30. R.A. Youg, A. Sakthivel, T.S. Moss and C.O. Paiva-Santos, "DBWS-9411 – an upgrade of the DBWS. Programs for Rietveld refinement with PC and mainframe computers", *J. Appl. Cryst.* **28**, 366–367 (1995).